RSC Advances

PAPER

Cite this: *RSC Adv.*, 2024, **14**, 139

Evaluation of physicochemical properties of citric acid crosslinked starch elastomers reinforced with silicon dioxide

Pooja N,[a] Ishita Chakraborty,[a] Sib Sankar Mal,[b] Alevoor Srinivas Bharath Prasad,[c] Krishna Kishore Mahato[a] and Nirmal Mazumder *[a]

Received 17th November 2023
Accepted 11th December 2023

DOI: 10.1039/d3ra07868j

rsc.li/rsc-advances

Thermoplastic starch (TPS), derived from renewable resources, offers advantages such as biodegradability and lower production costs compared to petroleum-based plastics. However, its limited mechanical properties pose a challenge for broader applications. This research aims to explore the potential of enhancing the mechanical and barrier properties of TPS films through the incorporation of silicon dioxide as a reinforcement filler and citric acid as a crosslinking agent. By introducing silicon dioxide as a reinforcement filler, the mechanical strength of the TPS films is expected to be improved. Additionally, the incorporation of citric acid as a crosslinking agent is anticipated to enhance the barrier properties of the films. The combination of these additives holds promise for creating TPS films with improved performance, contributing to the development of sustainable and environmentally friendly materials in various industries. The results reveal that SiO_2 improves the stiffness of the films at lower concentrations but causes brittleness at higher concentrations. In contrast, citric acid crosslinked films exhibit improved flexibility and density. Scanning electron microscopy demonstrates the morphological changes in the films, with SiO_2 affecting surface roughness and aggregate formation. SiO_2 reduces film thickness and transparency, while citric acid enhances water resistance and barrier properties. X-ray diffraction analysis shows a reduction in crystallinity due to the plasticization process. Fourier-transform infrared spectroscopy highlights chemical changes and antimicrobial activity is observed with citric acid against specific bacteria. The soil burial test reveals that citric acid crosslinked films exhibit slower degradation due to antimicrobial properties. The combination of SiO_2 reinforcement and citric acid crosslinking enhances the overall performance of the films, promising sustainable and environmentally friendly materials for various applications.

Introduction

Thermoplastic elastomers (TPEs) are a type of polymer that can be melted and molded multiple times without undergoing any significant changes in their chemical structure.[1] This allows for easy processing and recycling of TPEs, making them a more sustainable option for many applications. TPEs have a wide range of properties, including high flexibility, resilience, and excellent resistance to environmental factors such as heat, cold, and UV light. They are used in a variety of applications, including consumer goods, automotive parts, and medical devices.[2–4]

Thermoplastic starch (TPS) is a biodegradable and biocompatible material derived from renewable resources like corn, potato, or tapioca starch.[5,6] To produce TPS, granular starch undergoes thermomechanical treatment, which encompasses activities like kneading, extrusion, injection molding, compression molding, blow molding, or heating and casting in an excess water solution.[7,8] During this procedure, plasticizers such as water, glycerol, or urea, and additives like lecithin or monoglycerides are employed to enhance the material's properties.[9,10] One of the main challenges in using TPS is its limited mechanical properties compared to traditional petroleum-based plastics.[11] However, researchers are working to improve the properties of TPS through the addition of other biopolymers and fillers.[12–14] The thermoplastic characteristics of starch closely resemble those of synthetic polymers, allowing the adaptation of methods initially designed for synthetic polymers to be used in starch processing. This adaptability has resulted in the manufacture of commercial products made from TPS, which includes items like compost bags and packaging materials.[15] This material has several advantages over traditional petroleum-based plastics, including lower production costs, renewability, and biodegradability. It can be used in a variety of applications, such as packaging, agricultural mulch films, and food packaging materials.[16,17]

[a]*Department of Biophysics, Manipal School of Life Sciences, Manipal Academy of Higher Education, Manipal, Karnataka 576104, India. E-mail: nirmal.mazumder@manipal.edu*

[b]*Department of Chemistry, National Institute of Technology, Karnataka 575025, India*

[c]*Department of Public Health and Genomics, Manipal School of Life Sciences, Manipal Academy of Higher Education, Manipal, Karnataka 576104, India*

Overall, TPS is a promising alternative to traditional plastics in terms of sustainability and environmental impact, and its use is expected to grow in the coming years as demand for biodegradable and renewable materials continues to rise. The current work aims at using silicon dioxide as a reinforcement filler and citric acid as a crosslinking agent to potato starch. It is expected that the addition of silicon dioxide would enhance the mechanical properties, while citric acid would improve the barrier properties of the films.

Experimental section

Materials

Potato starch was acquired from Sigma Aldrich, USA. Glycerol (extrapure AR, 99.5%) and Silicon dioxide were supplied by Sisco Research Laboratories Pvt. Ltd., India. Citric acid anhydrous was obtained from Loba Chemie Pvt. Ltd., India. All the procured chemicals were of high-purity reagent grade.

Methods

Preparation of potato starch elastomers. Various batches of potato starch films containing 8 g potato starch were prepared by dissolving different amounts of silicon dioxide (SiO_2) (0.08 g, 0.16 g), citric acid (10%, 30%, and 50% w/w of potato starch), and a combination of both SiO_2 and citric acid in 100 mL of distilled water in a beaker. This method was adapted from our previous studies.[18,19] To prepare the potato starch elastomers, 4 mL of glycerol and acetic acid each was added to a beaker and mixed thoroughly. The beaker was then placed on a magnetic stirrer and heated to a temperature of 85–90 °C for approximately 45 min while being continuously stirred. The molten starch mixture was poured onto a casting tray carefully to avoid the formation of air bubbles and was allowed to dry in a hot air oven for 48 h at 60 °C. After drying, the biopolymer film was removed from the tray and stored in a controlled humidity chamber at a temperature of 37 °C and humidity above 50%.

Morphological characterization

Scanning electron microscopy (SEM). SEM (JEOL model JSM-6380LA system, Germany) was used to analyze the surface morphology of the biopolymer films. The starch films were cut into a 5 × 5 mm area and were coated with a thin layer of conductive material (gold) to ensure that the electrons from the SEM beam would be able to interact with the sample surface. The SEM was operated at 10 kV and 2000× magnification to visualize the surface topography of the starch films.

Structural characterization

Film thickness and transparency. The thickness of the prepared biopolymer films was measured using a Yuzuki digital micrometer with a resolution of 0.01 mm. Measurements were taken in five different regions of the films, and the mean value was calculated.

Transparency of the films was assessed by Thermo Fisher Scientific's Varioskan™ LUX multimode microplate reader, where 5 mm films were cut and placed at the bottom of the 96 well plate and the results were presented in terms of % transmittance. Transmittance, which measures the amount of light that passes through a sample at different wavelengths, was used as an indirect measure of transparency. Initially, the films' absorbance was measured for various wavelengths (300–700 nm). The following equation was employed to convert the absorbance values into % transmittance (%T).

$$\%T = \text{antilog}\,(2 - \text{absorbance}) \quad (1)$$

X-ray diffraction (XRD). The MiniFlex benchtop XRD system (Rigaku, Japan), was utilized to determine the starch films' crystallinity and amorphous content. Films measuring 2 cm in diameter were scanned with a step size of 0.02° over a range of 5–55° at a rate of 2° min^{-1}. Additionally, the instrument was employed to examine the material's bond angles and interatomic distance.

Chemical characterization

Fourier-transform infrared (FTIR) spectroscopy. To evaluate the chemical characteristics of the biopolymer films, their infrared spectra were captured using an attenuated total reflection (ATR) optics Fourier transform infrared spectrophotometer (Bruker alpha FTIR spectrometer, Germany) over a range of 400–4000 cm^{-1}. By transmitting radiation through the film, the molecular vibration of the specimen was accomplished. The film absorbed radiation at specific frequencies, leading to the formation of molecular vibrations. The absorption of frequencies provided data about the functional groups that were either established or broken during the preparation process.

Functional characterization

Water solubility. The initial weights (W_i) of 1 cm^2 biopolymer films were measured and dried at 105 ± 2 °C in the hot air oven overnight. Thereafter, the films were continuously stirred for 24 h while suspended in beakers containing 30 mL of distilled water. Filter paper was used to remove the surplus water from the films, and they were then dried for 24 h at 105 ± 2 °C. The films' final weights were noted as W_f. The percentage of water solubility was computed using the following equation:

$$\text{Water solubility} = \frac{W_i - W_f}{W_i} \times 100 \quad (2)$$

Moisture content. Determination of moisture content of starch films typically involves drying 3 cm^2 films in an oven at 60 °C overnight until a constant weight is obtained. The difference between the initial and final weights represents the amount of water that was present in the films. The moisture content is calculated by dividing the weight of water by the weight of the dry sample and multiplying by 100.

Water vapour permeability (WVP). The WVP of the films was assessed by cutting circular films 3 cm in diameter and firmly securing them around the opening of glass vials containing

10 mL of distilled water. The vials' initial weight was recorded. The setup was placed in a humidity chamber set to 40% relative humidity and 35 °C temperature for 24 h. To determine the amount of water vapour permeated through the films, the vials were removed and reweighed. The WVP of the films was calculated using the below-mentioned equation:

$$\mathrm{WVTR} = \Delta W\, A \times t \quad (3)$$

where ΔW is the weight loss in grams, A represents the cross-sectional area and t is time in h.

Universal testing machine (UTM). A Universal testing machine (Shimadzu Universal Texture Analyzer EZ SX) was used to evaluate the tensile strength of the starch elastomers. Specimens were cut into 90 mm length and 20 mm width. Three specimens of each film were tested considering the thickness of the individual films, and their mean value was reported as a force (N) *vs.* displacement (mm) plot.

Antimicrobial activity. The antimicrobial activity of the films was assessed by the Kirby–Bauer disc diffusion method on the Mueller Hinton agar (MHA) plate. ATCC strains of *Escherichia coli*, *Staphylococcus aureus*, and *Pseudomonas aeruginosa* were inoculated in a nutrient medium and incubated at 37 °C. Post incubation the bacterial cultures were then diluted to 0.5 McFarland with fresh nutrient medium and lawn culture of the various bacteria was made on MHA plates. The films were cut into a disc shape with 6 mm diameter. The discs containing known antibiotics were used as controls. The interpretation of the antimicrobial activity was done by measuring the diameters of the zones of inhibition around the films.

Biodegradation. The films were cut into 3 cm^2 pieces and were buried in pots filled with garden soil at a depth of 2 cm for 30 days in a greenhouse. The weight of the films was measured every ten days after soil burial. The biodegradability test was calculated by the equation below:

$$\text{Weight loss } (\%) = [(W_o - W)/(W_o)] \times 100$$

where W_o and W are the weights of samples before and after the test.

Results and discussion

Preparation of potato starch elastomers

The starch elastomers with different concentrations of SiO_2 and citric acid were prepared using solution casting technique. The inclusion of SiO_2 improved the stiffness of the film. At larger concentrations, however, the addition of SiO_2 caused brittleness. The citric acid crosslinked films showed improved flexibility and appeared denser than the rest of the films (Fig. 1).

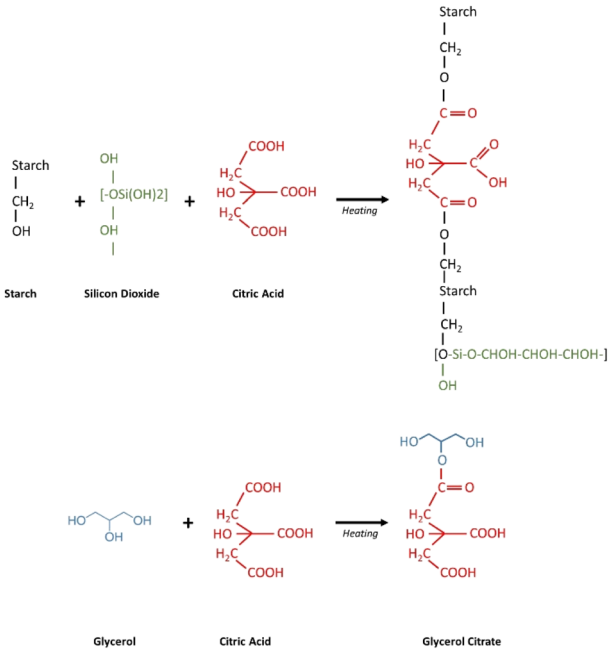

Fig. 1 Schematic representation of the mechanism of crosslinking of starch with silicon dioxide and citric acid.

Morphological characterization

Scanning electron microscopy. The SEM images (Fig. 2) provide a detailed examination of the morphology of potato starch elastomer films and reveal the impact of SiO_2 and citric acid on their surface characteristics. The potato starch elastomer film (Fig. 2a) exhibits an uneven surface with ungelatinized starch granules and cracks, a feature attributed to the inherent properties of potato starch. The addition of SiO_2 at low concentrations imparts a smooth surface with no visible aggregates (Fig. 2b), while at higher concentrations, an increase in roughness and the formation of silicon dioxide aggregates become apparent (Fig. 2c). This suggests that SiO_2, acting as a reinforcement filler, influences film morphology, enhancing smoothness at lower concentrations but causing roughness and aggregation at higher concentrations. Furthermore, citric acid-crosslinked films (Fig. 2d–f) display a homogeneous and smoother surface compared to potato starch and SiO_2-based

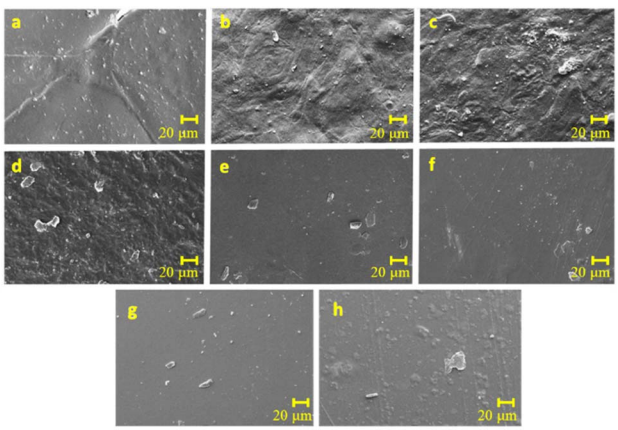

Fig. 2 Scanning electron microscope images of various potato starch elastomers (a) PS, (b) PS + 0.08 g SiO_2, (c) PS + 0.16 g SiO_2, (d) PS + 10% CA, (e) PS + 30% CA, (f) PS + 50% CA, (g) PS + 50% CA + 0.08 g SiO_2, (h) PS + 50% CA + 0.16 g SiO_2. PS: potato starch; SiO_2: silicon dioxide; CA: citric acid. Magnification: 500×; scale bar: 20 μm.

films. This indicates that citric acid has a leveling effect, contributing to a more uniform and refined film surface. Films containing both citric acid and SiO_2 (Fig. 2g and h) exhibit relatively smooth surfaces, suggesting a potential synergistic effect where the drawbacks associated with high SiO_2 concentrations, such as roughness, may be mitigated by the smoothing influence of citric acid. The observed uneven surface in the potato starch elastomer aligns with the granular nature of ungelatinized starch, potentially impacting the film's mechanical and barrier properties. The concentration-dependent effects of SiO_2 highlight the importance of optimizing its incorporation to achieve desired surface characteristics without compromising film quality. Citric acid's role in promoting a smoother and more homogeneous surface suggests its potential as a beneficial crosslinking agent in starch-based films. The combination of citric acid and SiO_2 appears to offer a balance, showcasing relatively smooth surfaces.

Structural characterization

Film thickness and transparency. The incorporation of SiO_2 reduced the thickness of the films, which could be attributed to the tightness and compactness of the polymeric matrix seen with its addition as a reinforcement filler (Table 1). The citric acid crosslinked films were visibly thicker since the film thickness was proportional to the total solid content of the formulation. Another study, conducted by Wu *et al.*, yielded comparable results, demonstrating a substantial increase in film thickness with the addition of citric acid.[20] Transmittance represents the transparency of the films. The transmittance (%) of various potato starch elastomers at wavelengths ranging from 300 to 700 nm is denoted in Fig. 3. The transparency of the films also improved with crosslinking and decreased with increasing concentration of SiO_2.

Table 1 Thickness (mm) of various potato starch elastomers

Starch elastomer	Thickness (mm)
PS	0.11 ± 0.02
PS + 0.08 g SiO_2	0.09 ± 0.03
PS + 0.16 g SiO_2	0.10 ± 0.03
PS + 10% CA	0.22 ± 0.04
PS + 30% CA	0.23 ± 0.01
PS + 50% CA	0.24 ± 0.04
PS + 50% CA + 0.08 g SiO_2	0.14 ± 0.03
PS + 50% CA + 0.16 g SiO_2	0.16 ± 0.03

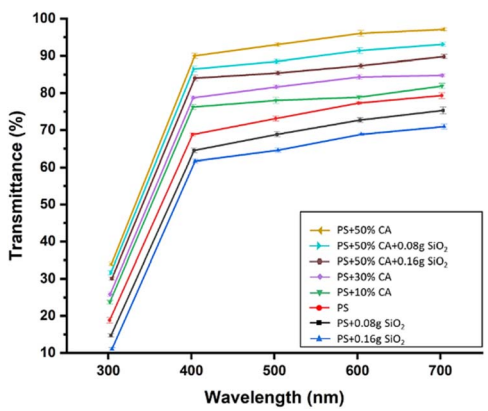

Fig. 3 Transmittance (%) of various potato starch elastomers at wavelengths ranging from 300 to 700 nm. PS: potato starch; SiO_2: silicon dioxide; CA: citric acid.

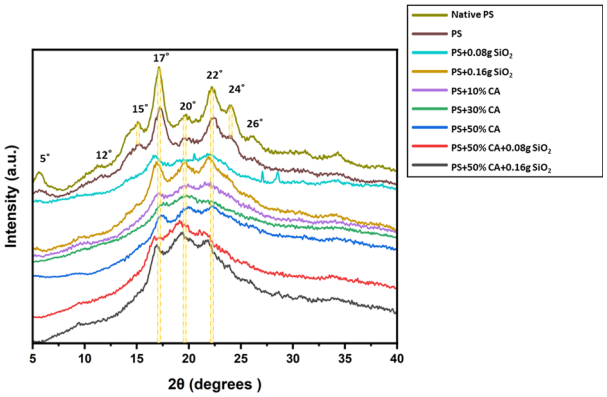

Fig. 4 X-ray diffractogram of various potato starch elastomers. PS: potato starch; SiO_2: silicon dioxide; CA: citric acid.

X-ray diffraction. XRD analysis determines the crystallinity of the developed elastomers. The X-ray diffractogram of various potato starch films is presented in Fig. 4. Starch consists of crystalline, semicrystalline, and amorphous domains. Potato starch is said to exhibit B-type crystallinity which comprises loosely packed double helical amylopectin moieties with a water molecule column at the center of the assembly. Peaks typical of B-type starch were visible in native potato starch at 5°, 12°, 15°, 17°, 20°, 22°, 24°, and 26°. A reduction in crystallinity was observed in all the potato starch elastomer films owing to the plasticization process *i.e.*, the addition of plasticizer, which is believed to disrupt the intermolecular hydrogen bonds present between the starch moieties.[10] The starch elastomers showed a form of crystalline form, consisting of reduced peaks at 17°, 20°, and 22°. Furthermore, crosslinking disrupts the regular arrangement of starch molecules, leading to a reduction in crystallinity. This disruption is attributed to the formation of covalent bonds, such as those formed between citric acid and starch molecules, which interfere with the intermolecular hydrogen bonds responsible for maintaining the crystalline structure. The result is the formation of amorphous regions within the film, contributing to an overall decrease in crystallinity.

Chemical characterization

Fourier-transform infrared (FTIR) spectroscopy. The FTIR spectra of various potato starch elastomers at 4000–600 cm^{-1} are shown in Fig. 5. All the elastomers show a similar spectrum consisting of a broad band appearing near 3340 cm^{-1} attributed to the OH group of the starch backbone. The other prominent peaks include the C–H, H–O–H, and C–O–C stretching vibration at 2930 cm^{-1}, 1650 cm^{-1}, and 990 cm^{-1} respectively. The C–O–C bend present at 1019 cm^{-1} in potato starch elastomer (PS), was

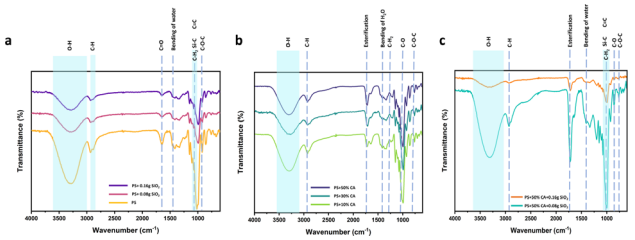

Fig. 5 FTIR spectra of various potato starch elastomers. (a) PS, PS + 0.08 g SiO_2, PS + 0.16 g SiO_2, (b) PS + 10% CA, PS + 30% CA, PS + 50% CA, (c) PS + 50% CA + 0.08 g SiO_2, PS + 50% CA + 0.16 g SiO_2. PS: potato starch; SiO_2: silicon dioxide; CA: citric acid.

observed to shift to higher wavenumbers with the addition of SiO_2 to potato starch.[21] The SiO_2 elastomers also displayed peaks at 1260 cm^{-1}, 1070 cm^{-1}, and 923 cm^{-1} which corresponded to Si–C, Si–O stretching, and Si–H bending vibrations. This could be attributed to the formation of intermolecular hydrogen bonds between SiO_2 and starch molecules. The citric acid crosslinked starch films showed the presence of a distinctive peak at 1724 cm^{-1} corresponding to ester group formation which thus confirms the crosslinking of citric acid and starch. The peak intensity was found to increase with increasing concentration of citric acid. In the study by Wu *et al.*, FTIR spectra also showed a peak at 1724 cm^{-1}, suggesting esterification between citric acid and starch. This peak intensity increased with higher concentrations of citric acid, indicating an increased crosslinking reaction.[20]

Functional characterization

Water solubility and moisture content. The water solubility and moisture content of various potato starch elastomers are shown in Fig. 6(a) and (b). The elastomers containing SiO_2 showed decreased water solubility and moisture content when compared to potato starch elastomers. The complex network formed by the intermolecular bonds between SiO_2 particles and starch could be attributed to the improvement in water resistance observed in the films. The addition of SiO_2 as reinforcement fillers also decreases the total void volume occupied by water molecules, thereby decreasing the moisture absorption and water solubility of the films. The addition of citric acid further enhances the water resistance of the films due to the strong hydrogen bonding formed between the carbonyl groups (C═O) and hydroxyl groups (OH) present in the molecular structure of citric acid and the hydroxyl groups in starch molecules. This bonding leads to the establishment of a cross-linking network, contributing to the development of a sturdier and more interconnected structure in the elastomers.

Water vapour permeability. A significant reduction in water vapour permeability was observed in SiO_2-reinforced and citric acid crosslinked films (Fig. 7). SiO_2, being a reinforcement filler material can increase the density and reduce the porosity of the film, making it more impermeable to gases and liquids. The formation of a network of cross-linking bonds within the starch matrix can reduce the size of the void spaces that allow water vapor to pass through.[22] This hypothesis is supported by the fact that both citric acid and SiO_2 can form chemical bonds with hydroxyl groups on the starch molecules, creating a more stable and cohesive film structure. Overall, the addition of citric acid and SiO_2 to starch films may have resulted in a more compact and less permeable material.

In their study, Ghanbarzadeh, Almasi, and Entezami aimed to enhance the barrier and mechanical properties of corn starch-based edible films. They investigated the impact of incorporating citric acid on these properties. The addition of citric acid had a positive effect, leading to improvements in the water resistance of the films.[23] Similar improvements in barrier properties were observed in our previous studies employing rice and potato starch, showcasing the versatility and effectiveness of citric acid as a crosslinking agent and SiO_2 as a reinforcement filler across different starch types.[19,24]

Mechanical properties. The mechanical properties of potato starch elastomers were evaluated through force *vs.* displacement graphs obtained from UTM analysis (Fig. 8). The graphs revealed significant insights into the materials' behavior under applied stress. The potato starch elastomer (PS) displayed an initial linear region indicating elastic deformation, followed by a peak point representing its tensile strength before undergoing plastic deformation and eventual failure. The incorporation of

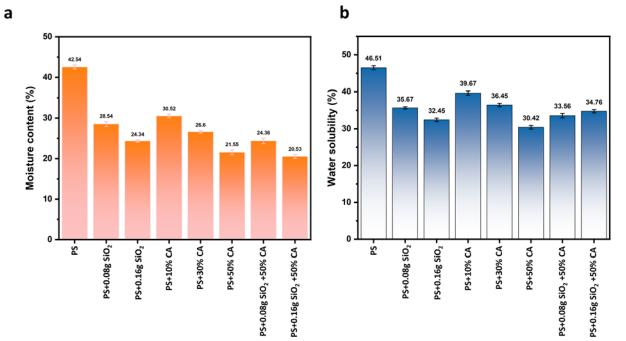

Fig. 6 (a) Water solubility (%), and (b) moisture content (%) of various potato starch biopolymer films. PS: potato starch; SiO_2: silicon dioxide.

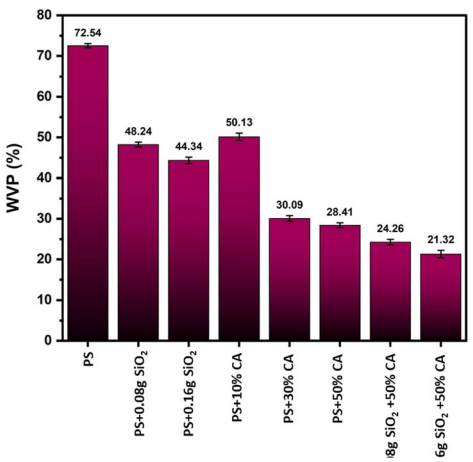

Fig. 7 Water vapour permeability (WVP) (%) of various potato starch biopolymer films. PS: potato starch; SiO_2: silicon dioxide.

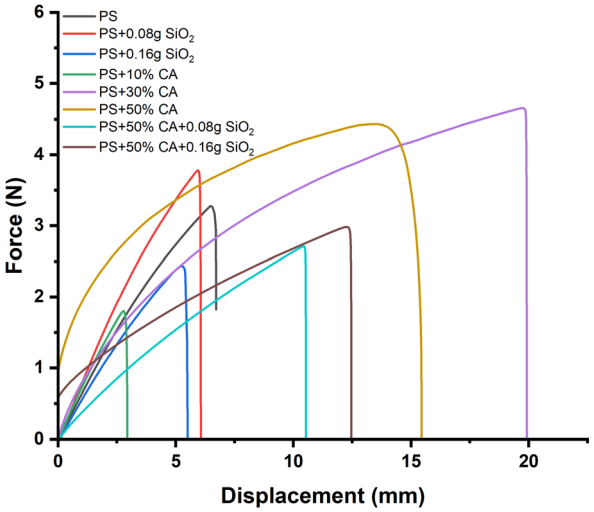

Fig. 8 Force *vs.* displacement graphs of different starch biopolymers (a) PS, (b) PS + 0.08 g SiO_2, (c) PS + 0.16 g SiO_2, (d) PS + 10% CA, (e) PS + 30% CA, (f) PS + 50% CA, (g) PS + 50% CA + 0.08 g SiO_2, (h) PS + 50% CA + 0.16 g SiO_2. PS: potato starch; SiO_2: silicon dioxide; CA: citric acid.

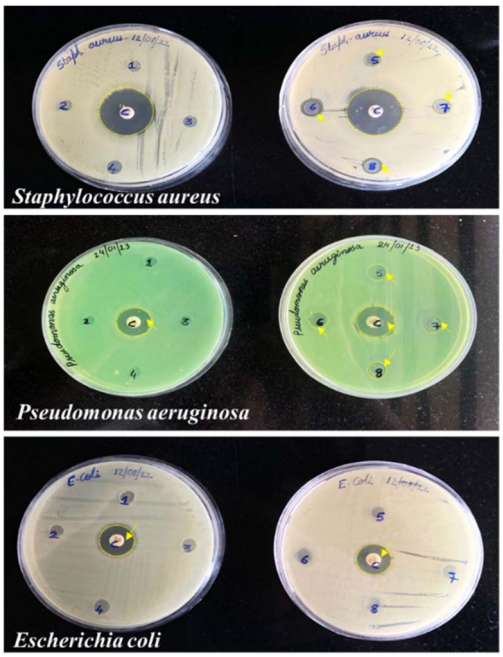

Fig. 9 MHA plates showing inhibition zones for various potato starch elastomers against *Staphylococcus aureus*, *Pseudomonas aeruginosa*, and *Escherichia coli*. (1) PS, (2). PS + 0.08 g SiO_2, (3) PS + 0.16 g SiO_2, (4) PS + 10% CA, (5) PS + 30% CA, (6) PS + 50% CA, (7) PS + 50% CA + 0.08 g SiO_2, (8) PS + 50% CA + 0.16 g SiO_2. C: control; PS: potato starch; SiO_2: silicon dioxide; CA: citric acid.

SiO_2 reinforcement increased the peak point, indicating improved tensile strength. While the initial addition of SiO_2 as a reinforcement filler led to an improvement in tensile strength, excessive amounts of SiO_2 resulted in a decrease in the material's mechanical properties. This reduction in tensile strength can be attributed to the films becoming brittle with higher concentrations of SiO_2. The brittleness indicates that the material's ability to undergo plastic deformation and absorb energy under stress was compromised, leading to a lower peak point on the force *vs.* displacement graph. As evident from the SEM images, higher concentrations of SiO_2 lead to formation of aggregates in the starch matrix. The presence of these aggregates interferes with the ability of the starch matrix to form a continuous and cohesive structure. The irregular distribution of SiO_2 can act as stress concentrators, leading to the initiation and propagation of microcracks within the film. The initiation of cracks at SiO_2 aggregates can reduce the effective load-bearing capacity of the film, ultimately resulting in a decrease in tensile strength. Crosslinking the PS elastomer with citric acid further enhanced the peak point, demonstrating stronger mechanical properties. However, increased concentrations of citric acid can cause degradation of starch, causing a decrease in the mechanical strength of the films. These findings align with several studies that employed citric acid as a crosslinking agent. Simões *et al.* prepared hydrogel films from cassava starch, xanthan gum, glycerol, and citric acid using extrusion. They investigated the effects of citric acid concentration (0–6% w/w) as a crosslinking agent on the tensile strength of the hydrogel films. Incorporating citric acid as a crosslinker resulted in hydrogel films with higher tensile strength and lower elongation. The most pronounced improvements in tensile strength were observed as citric acid concentration increased from 0% to 4% w/w. Higher citric acid concentrations (>4% w/w) promoted degradation of the polymeric chains, reducing tensile strength.[25] The combination of SiO_2 reinforcement and citric acid crosslinking resulted in the highest peak point, signifying the most improved tensile strength among all the elastomers. These findings highlight the potential of creating TPS films with superior mechanical performance through the synergistic effect of SiO_2 reinforcement and citric acid crosslinking, contributing to the development of sustainable and environmentally friendly materials.

Antimicrobial activity. The zone of inhibition was assessed by determining the diameter of microbial inhibition around the films. The addition of SiO_2 was found to show no effect on the antimicrobial properties of the films. However, citric acid was

Table 2 Inhibition zones for various potato starch elastomers against Gram-positive and Gram-negative bacteria. C: control; PS: potato starch; SiO_2: silicon dioxide; CA: citric acid

		Zone of inhibition (mm)		
		S. aureus	*P. aeruginosa*	*E. coli*
C	Cefuroxime	26	NA	16
	Ceftazidime	NA	19	NA
1	PS	—	—	—
2	PS + 0.08 g SiO_2	—	—	—
3	PS + 0.16 g SiO_2	—	—	—
4	PS + 10% CA	—	—	—
5	PS + 30% CA	7	8	—
6	PS + 50% CA	11	9	—
7	PS + 50% CA + 0.08 g SiO_2	8	8	—
8	PS + 50% CA + 0.16 g SiO_2	7	8	—

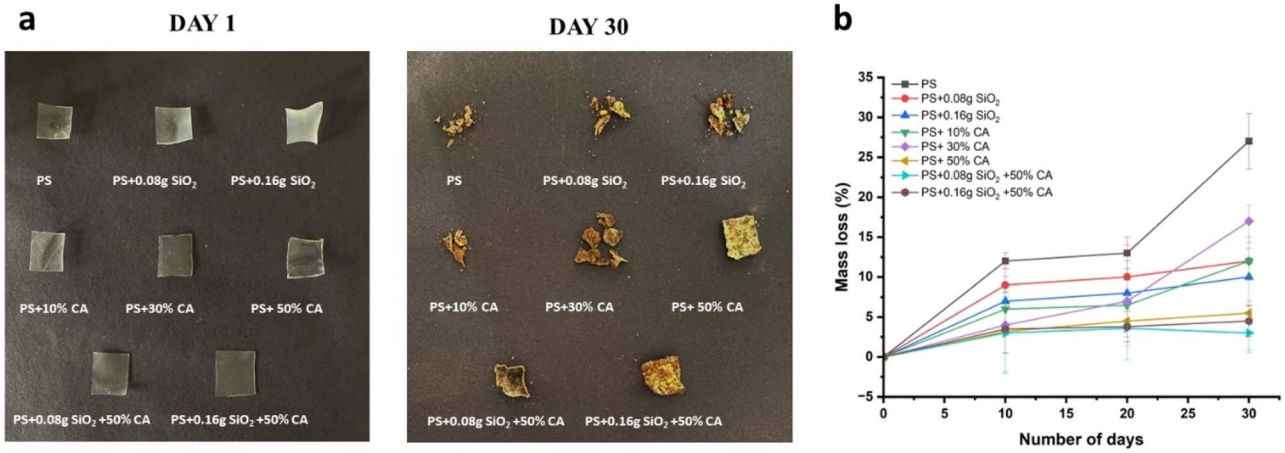

Fig. 10 (a). Photographs of potato starch elastomers at day 1 and day 30 of soil burial test; (b) Weight loss (%) curve exhibiting biodegradation of elastomers in garden soil.

observed to possess antimicrobial activity against *Staphylococcus aureus* and *Pseudomonas aeruginosa*. Antimicrobial activity increased with increasing concentration of citric acid with 50% CA showing the highest zone of inhibition. This can be attributed to the acidic nature of citric acid which can rupture the cell membrane of the bacteria. The inhibition zones (mm) of different potato starch films against *Escherichia coli*, *Staphylococcus aureus*, and *Pseudomonas aeruginosa*, are depicted in Fig. 9 and Table 2. This observation is in alignment with a study that evaluated the inhibitory effects of citric acid crosslinking on the growth of *Staphylococcus aureus* and *Escherichia coli*. It was observed that the diameter of inhibition zones increased with the concentration of citric acid, indicating its inhibitory effects on bacteria.[20]

Biodegradation. The soil burial method is a common approach to investigate the biodegradation of starch films. In this method, the starch films are buried in the soil for a certain period of time, during which the microorganisms present in the soil break down the films. The rate of biodegradation can be determined by periodically retrieving the films from the soil, cleaning them to remove any soil debris, and measuring their weight loss, mechanical properties, and/or chemical changes. The extent of biodegradation can also be assessed by examining the morphology of the films using microscopy techniques. The soil burial method is often used to evaluate the biodegradability of starch films and other biodegradable materials under natural environmental conditions. Photographs of potato starch elastomers on day 1 and day 30 of the soil burial test and their subsequent weight loss (%) are depicted in Fig. 10. The introduction of silicon dioxide as an additive did not yield any significant effects on the degradation of elastomers. In other words, the presence of silicon dioxide did not noticeably influence or alter the deterioration process of the elastomer material. On the other hand, when films were crosslinked using citric acid, a different outcome was observed. These citric acid crosslinked films exhibited slower rates of degradation compared to their counterparts.

This decelerated degradation can be attributed to the antimicrobial activity exhibited by citric acid. The antimicrobial properties of citric acid play a crucial role in slowing down the degradation process. By inhibiting the growth of microorganisms, citric acid effectively delays the onset of microbial activity on the elastomer material. Consequently, this delay in microbial growth results in a decelerated degradation process, effectively extending the lifespan or durability of the elastomer material. Mali *et al.* examined the biodegradation of yam starch films incorporating citric acid *via* soil burial for up to 60 days.[26] Consistent with our present findings, the incorporation of citric acid in the crosslinking process resulted in a decelerated rate of biodegradation. The outcome mirrored our current observations, indicating that the crosslinked films exhibited reduced biodegradation rates. This phenomenon was linked to the more compact structure of the films, limiting microbial access, and impeding their degradative activity.

Conclusion

While previous studies have individually investigated the effects of SiO_2 or citric acid on TPS films, our research is among the first to comprehensively examine the combined impact of these two additives. The synergistic action of SiO_2 and citric acid is particularly innovative in enhancing the mechanical, barrier, and antimicrobial properties of the TPS films. SiO_2 acts as a reinforcement filler, influencing film morphology and improving mechanical strength, while citric acid serves as a crosslinking agent, contributing to enhanced flexibility and reduced water solubility. The combination of these additives has demonstrated a balancing effect, mitigating the drawbacks associated with high SiO_2 concentrations, such as roughness, through the smoothing influence of citric acid.

Furthermore, our study delves into the antimicrobial activity of the films, revealing the potential of citric acid to effectively inhibit microbial growth, thus extending the shelf life of packaged products and offering applications in areas such as food

packaging and biomedical sectors. The optimization of silicon dioxide and citric acid concentrations is crucial to achieving the desired balance between mechanical strength and flexibility in the films. By further exploring and fine-tuning these parameters, the performance of TPS films can be enhanced, expanding their potential applications as eco-friendly alternatives to traditional petroleum-based plastics.

Author contributions

Pooja N: data curation; investigation; visualization; methodology; writing – original draft. Ishita Chakraborty: data curation; writing – original draft. Sib Sankar Mal: supervision, writing – review & editing. Bharath Prasad A: methodology; writing – review & editing. Krishna Kishore Mahato: supervision; review & editing. Nirmal Mazumder: conceptualization; supervision; review & editing.

Conflicts of interest

The authors declare no conflict of interest.

Acknowledgements

NM thanks the Science and Engineering Research Board (SERB) (project number: MTR/2020/000058), Department of Science and Technology, Government of India, and Indian Council of Medical Research (ICMR), (Project Number-ITR/Ad-hoc/43/2020-21, ID No. 2020-3286) Government of India, India and the Global Innovation and Technology Alliance (GITA), Department of Science and Technology (DST), India [Project Number-GITA/DST/TWN/P-95/2021], for financial support. NM thanks the Manipal School of Life Sciences, Manipal Academy of Higher Education (MAHE), Manipal, Karnataka, India for providing the infrastructure and facilities. PN thanks MAHE, Manipal, Karnataka, India for the Dr T. M. A. Pai PhD fellowship.

References

1 J. P. Sheth, J. Xu and G. L. Wilkes, *Polymer*, 2003, **44**, 743–756.
2 E. Roy, J. C. Galas and T. Veres, *Lab Chip*, 2011, **11**, 3193–3196.
3 R. Shaker and D. Rodrigue, *Appl. Sci.*, 2019, **9**, 1–20.
4 O. P. Grigoryeva, A. M. Fainleib, A. L. Tolstov, O. M. Starostenko, E. Lievana and J. Karger-Kocsis, *J. Appl. Polym. Sci.*, 2005, **95**, 659–671.
5 E. M. N. Polman, G. J. M. Gruter, J. R. Parsons and A. Tietema, *Sci. Total Environ.*, 2021, **753**, 141953.
6 N. Pooja, S. Banik, I. Chakraborty, S. S. Mal, K. K. Mahato, P. Srisungsitthisunti and N. Mazumder, *Laser Science*, Optica Publishing Group, 2021, JW7A. 73.
7 Y. Zhang and C. Rempel, *Thermoplast. Elastomers*, 2012, 118119.
8 R. Thakur, P. Pristijono, C. J. Scarlett, M. Bowyer, S. P. Singh and Q. V. Vuong, *Int. J. Biol. Macromol.*, 2019, **132**, 1079–1089.
9 M. L. Sanyang, S. M. Sapuan, M. Jawaid, M. R. Ishak and J. Sahari, *Polymers*, 2015, **7**, 1106–1124.
10 Z. Y. Ben, H. Samsudin and M. F. Yhaya, *Eur. Polym. J.*, 2022, **175**, 111377.
11 Y. Zhang, C. Rempel and Q. Liu, *Crit. Rev. Food Sci. Nutr.*, 2014, **54**, 1353–1370.
12 P. Balakrishnan, S. Gopi, M. S. Sreekala and S. Thomas, *Starch/Staerke*, 2018, **70**, 1–34.
13 M. S. Maulida and P. Tarigan, *J. Phys. Conf. Ser.*, 2016, **710**, 012012.
14 T. Mekonnen, P. Mussone, H. Khalil and D. Bressler, *J. Mater. Chem. A*, 2013, **1**, 13379–13398.
15 G. Coppola, M. T. Gaudio, C. G. Lopresto, V. Calabro, S. Curcio and S. Chakraborty, *Earth Syst. Environ.*, 2021, 231–251.
16 M. K. Marichelvam, M. Jawaid and M. Asim, *Fibers*, 2019, **7**, 1–14.
17 R. Shi and B. Li, *Starch/Staerke*, 2016, **68**, 1224–1232.
18 N. Pooja., S. Banik, I. Chakraborty, S. S. Mal, K. K. Mahato, P. Srisungsitthisunti and N. Mazumder, Microscopic and Thermal Characterization of Starch-Silicon Dioxide Elastomers, *Frontiers in Optics + Laser Science*, 2023, JTu5A.8.
19 I. Chakraborty, N. Pooja, S. Banik, I. Govindaraju, K. Das, S. S. Mal, G. Y. Zhuo, M. A. Rather, M. Mandal, A. Neog, R. Biswas, V. Managuli, A. Datta, K. K. Mahato and N. Mazumder, *J. Appl. Polym. Sci.*, 2022, **139**, 1–12.
20 H. Wu, Y. Lei, J. Lu, R. Zhu, D. Xiao, C. Jiao, R. Xia, Z. Zhang, G. Shen, Y. Liu, S. Li and M. Li, *Food Hydrocoll.*, 2019, **97**, 105208.
21 S. Tang, P. Zou, H. Xiong and H. Tang, *Carbohydr. Polym.*, 2008, **72**, 521–526.
22 S. Yao, B. J. Wang and Y. M. Weng, *Food Packag. Shelf Life*, 2022, **32**, 100845.
23 B. Ghanbarzadeh, H. Almasi and A. A. Entezami, *Ind. Crops Prod.*, 2011, **33**, 229–235.
24 N. Pooja, S. Banik, I. Chakraborty, S. S. Mal, K. K. Mahato, P. Srisungsitthisunti and N. Mazumder, *Opt. InfoBase Conf. Pap.*, 2021, 6–7.
25 B. M. Simões, C. Cagnin, F. Yamashita, J. B. Olivato, P. S. Garcia, S. M. de Oliveira and M. V. Eiras Grossmann, *LWT*, 2020, **125**, 108950.
26 S. Mali, M. V. E. Grossmann, M. A. García, M. N. Martino and N. E. Zaritzky, *J. Food Eng.*, 2006, **75**, 453–460.